

# Recent Progress in Short-Wavelength VCSEL-Based Optical Interconnections

Rainer Michalzik<sup>\*a</sup>, Hendrik Roscher<sup>a</sup>, Martin Stach<sup>a</sup>, Dieter Wiedenmann<sup>\*\*b</sup>,  
Michael Miller<sup>b</sup>, Jes Broeng<sup>+c</sup>, Anders Petersson<sup>c</sup>, Niels A. Mortensen<sup>c</sup>,  
Harald R. Simonsen<sup>c</sup>, and Erhard Kube<sup>++d</sup>

<sup>a</sup>University of Ulm, Optoelectronics Department, D-89069 Ulm, Germany

<sup>b</sup>U-L-M photonics GmbH, Lise-Meitner-Str. 13, D-89081 Ulm, Germany

<sup>c</sup>Crystal Fibre A/S, Blokken 84, DK-3460 Birkerød, Denmark

<sup>d</sup>LightPointe Europe GmbH, Werkstättenstr. 16, D-01157 Dresden, Germany

## ABSTRACT

We report on recent progress in the design and application of vertical-cavity surface-emitting lasers (VCSELs) for optical interconnect applications in the 850 nm emission wavelength regime. Ongoing work toward parallel optical interconnect modules with channel data rates of 10 Gbit/s is reviewed and performance results of flip-chip integrated two-dimensional VCSEL arrays are presented. 10 Gbit/s speed as well as low thermal resistance of the lasers has been achieved. As a possible alternative to graded-index multimode fibers, we show 10 Gbit/s data transmission over 100 m length of a novel, entirely undoped multimode photonic crystal fiber. The use of VCSELs with output powers in the 10 mW range is demonstrated in a 16-channel free-space optical (FSO) module and VCSELs with even higher output power are shown to provide possible FSO connectivity up to data rates of 2.5 Gbit/s.

**Keywords:** Surface-emitting lasers, VCSELs, semiconductor laser arrays, optical interconnections, photonic crystal fiber, micro-structured fiber, 10-Gigabit Ethernet, free-space optics, optical wireless communications

## 1. INTRODUCTION

VCSELs emitting in the short-wavelength spectral regime centered at 850 nm continue to be the light source of choice for optical interconnects based on multimode fibers or high-speed free-space optical links. The latter may provide convenient data access over distances in the kilometer range and are increasingly attracting interest. The present paper is meant to complement a recent publication,<sup>1</sup> in which we have dealt with the use of gain-switched single-mode and multimode VCSELs for differential mode delay measurements of high-bandwidth graded-index multimode fibers (MMFs), 10 Gbit/s data transmission over low-loss polymer waveguides for optical backplane applications, first implementations of flip-chip integrated 8×8 VCSEL arrays, an introduction to FSO technology, as well as the principal design of a multi-beam transmitter for increased link availability.

With regard to two-dimensional (2-D) VCSEL arrays, in this paper we demonstrate 10 Gbit/s operation of single channels and a drastic reduction of the lasers' thermal resistance through optimized placement of the bonding pads. In the free-space section, we report on successful field trials with actual multi-beam devices and the static and dynamic characterization of large-area, high-power VCSELs. As for multimode fiber links, for the first time we show VCSEL-based data transmission over as much as 100 m of a 50 μm core diameter photonic crystal fiber (PCF).

---

Further author information: (Send correspondence to Rainer Michalzik)

\* E-mail: rainer.michalzik@e-technik.uni-ulm.de; phone +49-731-5026048; fax +49-731-5026049;  
<http://www-opto.e-technik.uni-ulm.de/>

\*\* E-mail: dieter.wiedenmann@ulm-photonics.de; <http://www.ulm-photonics.de/>

+ E-mail: jb@crystal-fibre.com; <http://www.crystal-fibre.com/>

++ E-mail: ekube@lightpointe.com; <http://www.lightpointe.com/>

## 2. TOWARD 10 GBIT/S PARALLEL OPTICAL INTERCONNECT MODULES

Perhaps the most important recent step ensuring a long-lasting presence of 850 nm VCSELs in the local area networking segment has been the adoption of a VCSEL–MMF link solution into the 10-Gigabit Ethernet (10-GbE) standard.<sup>2</sup> In 10-GbE, short-wavelength options exist for the transport of 10 Gbit/s signals over either up to 65 m of regular quality (bandwidth–length product  $BLP = 500 \text{ MHz} \cdot \text{km}$ ) MMF or up to 300 m of 850 nm bandwidth-optimized ( $BLP \geq 2 \text{ GHz} \cdot \text{km}$ ) MMF, both with 50  $\mu\text{m}$  core diameter. Higher bandwidth density on the card edges of high-performance switch and router platforms is most cost-effectively achieved by employing the space division multiplexing scheme, where a linear monolithic array of VCSELs with typically 250  $\mu\text{m}$  pitch is connected to a corresponding photodiode array by means of a MMF ribbon cable terminated by compact multi-fiber connectors. This approach is often referred to as a parallel optical interconnect (POI). A particularly comprehensive overview over the POI scene can be obtained through an online forum<sup>3</sup> in which relevant data of most (and sometimes previous) products are collected. Whereas several companies are able to supply transceivers with up to about  $12 \times 3 \text{ Gbit/s}$  aggregate throughput, to date no complete solution with channel data rates of 10 Gbit/s has been presented. While progress in this field is somewhat delayed owing to the overall market situation fostering reserved customer attitudes, it is also true that significant technical challenges have to be overcome with respect to, e.g., electrical crosstalk and impedance matching, both in the design of the transmitter side<sup>4</sup> and the receiver side.<sup>5</sup> At the time of writing (early August 2003), recent publications on 10 Gbit/s POI links still have the status of press releases.

At the exhibition accompanying the Optical Fiber Communication Conference (OFC) in Atlanta, GA, USA in March 2003, Picolight, Inc. and IBM have presented results of a  $12 \times 10 \text{ Gbit/s}$  experiment<sup>6</sup> making use of Picolight's high-speed 850 nm VCSEL arrays and IBM's silicon germanium VCSEL driver circuits and custom-built parallel test equipment.<sup>4</sup> Open eye diagrams at 10.3125 Gbit/s data rate were shown for parallel operation of all 12 channels using pseudo-random bit sequence (PRBS) non-return-to-zero (NRZ) modulation with  $2^{31} - 1$  word length.

At the same event, a group of four companies has reported on  $12 \times 10 \text{ Gbit/s}$  POI operation over 300 m of high-performance MMF.<sup>7</sup> In this case, the reliability-tested VCSEL arrays were supplied by U-L-M photonics, Primarion had fabricated the VCSEL driver and optical receiver arrays, Microsemi contributed the monolithic pin-type GaAs-based detector arrays, and the employed LaserWave<sup>TM</sup> 300 fiber is a product of OFS, the former optical fiber solutions division of Lucent Technologies.

Since the successful operation of all critical components has been demonstrated, based on the above pioneering work it can be expected that with some additional engineering effort, POI modules will become commercially available as soon as actual market demand arises.

## 3. FLIP-CHIP INTEGRATED TWO-DIMENSIONAL 850 NM VCSEL ARRAYS

As an obvious extension of the POI modules from Sect. 2 based on one-dimensional VCSEL arrays, substrate side emitting 2-D arrays<sup>8,9</sup> enable the low-cost fabrication of optical short-reach transmitters with very high channel count and channel densities far exceeding  $1000 \text{ ch/cm}^2$ . From the technological point of view, the arrays are widely scalable and therefore allow for a multiplication of the serial data rates of targeted 10 Gbit/s in order to reach very high aggregate bandwidths of well into the Tbit/s regime.

### 3.1. Array Fabrication and Operation Behavior

We have hybridized  $8 \times 8$  and  $4 \times 8$  arrays of 850 nm oxide-confined VCSELs with 250  $\mu\text{m}$  device pitch directly onto silicon fanout chips by means of an indium solder based flip-chip technology. During the high temperature bonding process, the restoring force exerted by the surface tension of the molten solder moves the VCSEL array into a nearly perfectly aligned position. Up to 100% bonding yield was achieved. For the light generated in the GaAs active region of the bottom-emitting VCSELs to be able to actually escape, the GaAs substrate, which is highly absorptive at the operating wavelength, has to be removed. All that remains of the wafer is an epitaxial layer of only about 3  $\mu\text{m}$  thickness connecting the VCSEL mesas. A photograph of a completed 64-channel module is shown in Fig. 1. The topography of the VCSEL's bottom surface is recognizable and

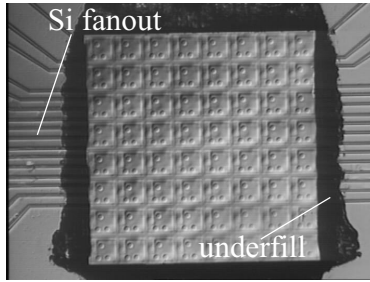


**Figure 1.** Top view of a 64-channel array hybridized onto a Si fanout.

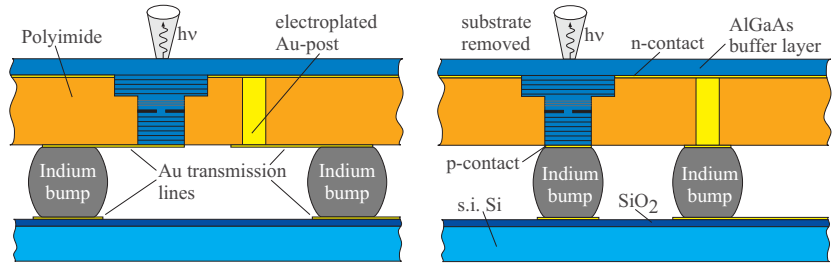


**Figure 2.** Illustration of the offset-bonded (*left*) and the direct-bonded (*right*) VCSEL design.

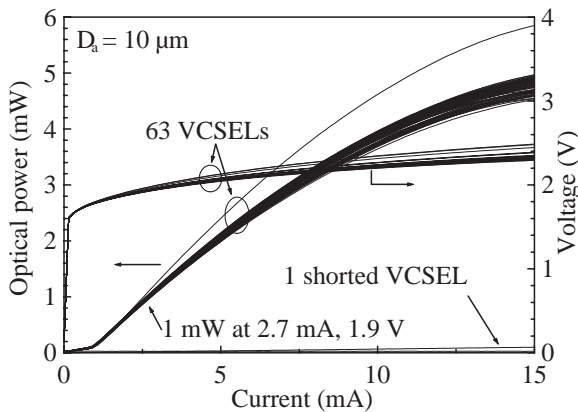


**Figure 3.** CW operation characteristics of all 64 VCSELs with  $D_a = 10 \mu\text{m}$  aperture size of an offset-bonded array.

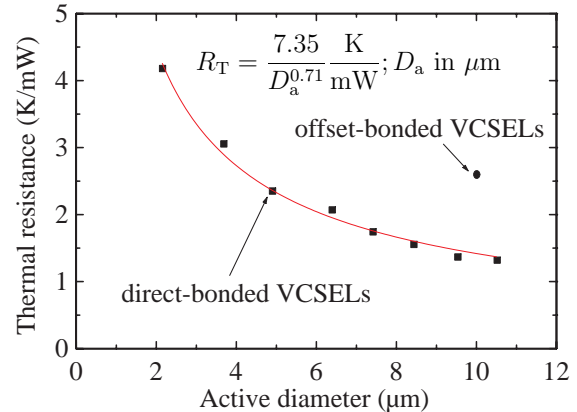


**Figure 4.** Measured thermal resistances for various aperture sizes of the direct-bonded VCSELs, and for offset-bonded VCSELs with  $D_a = 10 \mu\text{m}$ .

each  $250 \times 250 \mu\text{m}^2$  cell in the array can be distinguished. The dark frame surrounding the array is the cured underfill employed to provide mechanical stability and to protect the chip during the substrate removal process.

Two different VCSEL structures were implemented. The offset-bonded design on the left-hand side of Fig. 2 has a gold metallization of  $3 \mu\text{m}$  thickness connecting the n- and p-contacts laterally to the bonding pads over a distance in the order of  $100 \mu\text{m}$ . This was implemented in the early stages of development of this flip-chip technology out of concerns regarding bond pad stability (e.g. adhesion to the non-wettable layer, penetrability by the molten solder or its effectiveness as diffusion barrier for the solder material), bump size control (affecting bonding yield), and the choice of solder material (hard vs. soft solder). The design insures that the n- and p-bonding pads are fabricated on a perfectly even surface, are at exactly the same elevation, and are far enough from the mesas, so no stresses arising from coefficient of thermal expansion mismatch of the joined substrates could be induced into the active structures. The L-I-V (light-current-voltage) curves for an  $8 \times 8$  array in Fig. 3 exhibit rather good homogeneity except for one device with substantially enhanced output power for unclear reasons. The shorted VCSEL could well be caused by a faulty transmission line on this particular early fabricated Si fanout chip. Lasing of the  $10 \mu\text{m}$  current aperture devices sets in consistently at  $1 \text{ mA}$  current and  $1.8 \text{ V}$  applied voltage. An optical output power of  $1 \text{ mW}$  is reached at  $2.7 \text{ mA}$  and  $1.9 \text{ V}$ . The lateral offsets in this design, however, hamper the heat transport within the structure and result in a fairly high thermal resistance of  $R_T = 2.6 \text{ K/mW}$  for  $10 \mu\text{m}$  diameter lasers, as reported in [1]. This leads to a drastic junction temperature ( $T_j$ ) rise during operation, e.g.  $\Delta T_j \approx 50 \text{ K}$  at  $10 \text{ mA}$  laser current, which causes a pronounced red-shift of the output spectrum and generally shortens the lifetime of these devices.

### 3.2. Reduction of the Thermal Resistance

The development of reliable bonding pads, the use of soft indium solder, and precise bump size control facilitated the direct-bonded design shown on the right-hand side of Fig. 2, similar to the approach used in [10]. For technological reasons, this design involves different bump sizes for the n- and p-bumps to accommodate uneven bonding pads at slightly different mean elevations (omitted in the above figure). The elimination of thermal bottlenecks with the direct-bonded design cuts the thermal resistance by half (about 1.3 K/mW for 10 to 10.5  $\mu\text{m}$  devices), yet there still seems to be room for improvements. Lifetime investigations for VCSELs of the same type indicate that the lifetime doubles for every 20 K drop in internal temperature. Figure 4 gives more data for the 8 different sizes fabricated within a  $4 \times 8$  array of direct-bonded VCSELs. Due to the modified heat flow path, the functional fit  $R_T = R_T(D_a)$  included in the figure does not quite conform to the well-known<sup>11</sup> dependence  $R_T \propto D_a^{-1}$  observed in top-emitting VCSELs with heat removal from the substrate side.

### 3.3. Small-Signal and Digital Modulation Characteristics

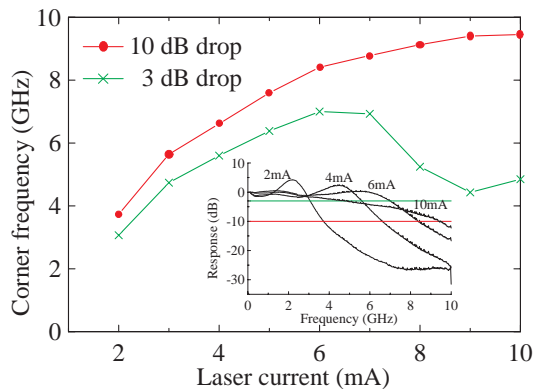


**Figure 5.** Small-signal 3-dB and 10-dB bandwidth as a function of operating current (offset-bonded design). Inset: The bias-dependent transfer functions.

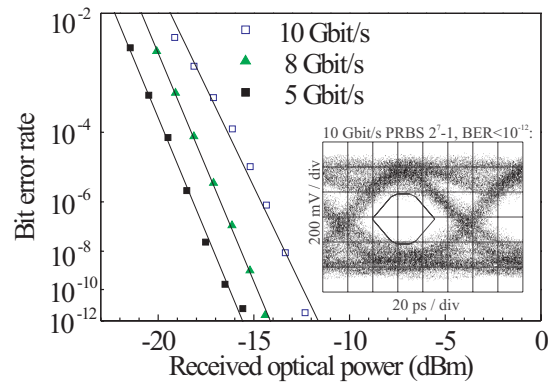


**Figure 6.** Bit error rate (BER) characteristics of the offset-bonded VCSELs and eye diagram at 10 Gbit/s data rate, using 6.5 mA bias and  $V_{pp} = 0.65$  V modulation.

In order to obtain modulation characteristics of the flip-chip bonded VCSELs, coplanar transmission lines are provided on the fanouts allowing for individual addressing of the array's elements. Low loss contacts were established to the approximately 7 mm long lines using commercial microwave probe heads. The modulated light is detected by a photoreceiver and recorded with an RF spectrum analyzer or sampling oscilloscope after low noise amplification. The transfer functions displayed in the inset of Fig. 5 indicate maximum small-signal 3-dB and 10-dB bandwidths of 7 GHz at 6 mA and 9.4 GHz at 10 mA of operating current, respectively. Note that the photoreceiver has a 3-dB bandwidth of 8 GHz. Digital data transmission experiments were conducted using that same setup. The curves in Fig. 6 demonstrate that quasi error-free (bit error rate  $< 10^{-12}$ ) 10 Gbit/s transmission was achieved. There is no indication of a noise floor or saturation behavior. Although the present eye opening does not entirely conform to the indicated mask according to the IEEE 802.3ae 10-Gigabit Ethernet standard,<sup>2</sup> we see much room for improvement through optimization of the fanout design and VCSEL dynamics.

## 4. DATA TRANSMISSION OVER PHOTONIC CRYSTAL FIBERS

Optical datacom systems as employed for the high-speed interconnection of electronic sub-systems rely on either simple large core diameter step-index fibers or graded-index multimode fibers. Due to strong inter-modal dispersion, the use of the former fiber type is limited to link lengths of some meters at Gbit/s data rates while fabrication of the latter requires tight control over the refractive index profile. This is particularly true for optimized 50  $\mu\text{m}$  core diameter fibers enabling up to 300 m serial transmission of 10 Gbit/s signals, as defined in [2]. Since optical interconnect requirements move toward higher speed over shorter distances, the availability of an easily manufacturable, yet high-speed capable fiber medium would be very beneficial. In what follows

we report on the properties of a new type of multimode photonic crystal fiber (PCF) with relatively simple waveguide geometry and demonstrate 850 nm data transmission at 10 Gbit/s over as much as 100 m length.

#### 4.1. Parameters of the Photonic Crystal Fiber

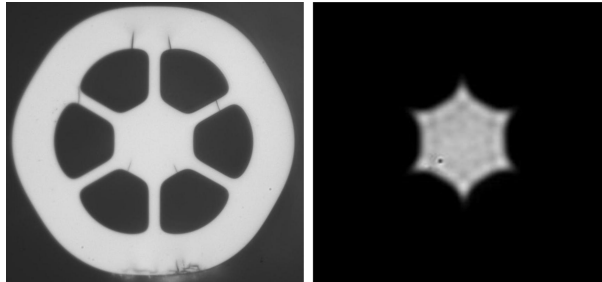


**Figure 7.** Cross-sectional view of a multimode photonic crystal fiber (*left*) and typical near-field pattern (*right*).

The design of the new multimode photonic crystal fiber is illustrated on the left-hand side of Fig. 7. The fiber is made from a single undoped material and it comprises a solid, pure silica core suspended in air by narrow silica bridges. Despite the zero index step between the core and the bridges, the fiber is capable of guiding light with good confinement to the multimode core, which can be inferred from the near-field distribution on the right-hand side of Fig. 7. The waveguiding properties of the fiber may accurately be tailored by adjusting parameters such as the size and shape of the core, the dimensions and number of silica bridges, or the fiber material. The numerical aperture (NA) of this type of PCF is essentially determined by the width of the silica bridges relative to the wavelength.<sup>12</sup> In this paper we focus on two fibers with 33 and 50  $\mu\text{m}$  core diameter and bridge widths of 4.8 and 7.0  $\mu\text{m}$ , respectively, yielding  $\text{NA} \approx 0.07$  and 0.05 at 850 nm wavelength.

Assuming worst-case conditions,<sup>13</sup> we estimate from the NA figures a bit rate–length product of around 350 Mbit/s · km for the 50  $\mu\text{m}$  fiber, whereas the 33  $\mu\text{m}$  sample should be inferior by about a factor of two. In the following sections we examine the transmission properties of such PCFs with 100 m length.

#### 4.2. Small-Signal Transfer Function and Differential Mode Delay Measurements

In order to get a first indication of the fibers' expected transmission bandwidths, we have determined the small-signal frequency responses with a scalar network analyzer. As optical source, standard 850 nm GaAs-based VCSELs have been employed. The 12  $\mu\text{m}$  active diameter oxide-confined devices show transverse multimode emission with a root mean square spectral width of less than 0.4 nm even under modulation. The lasing threshold current amounts to 1.8 mA and the bias current for the small-signal as well as data transmission experiments was chosen as 9 mA, where the 3-dB bandwidth is 8.6 GHz. At the receiving end, a multimode fiber pigtailed InGaAs pin-photoreceiver with above 8 GHz bandwidth was used. Figure 8 depicts the relative responses of both PCF samples. The 33 and the 50  $\mu\text{m}$  core diameter fiber show a bit rate–length product of 200 and 430 MHz·km, respectively. Though these figures have the approximate one-to-two correspondence expected from the corresponding NA's, their magnitudes are considerably higher than estimated above. To explain this, we note that in general the bit rate–length product is very dependent on the particular modal distribution of delay times and attenuation coefficients, as well as the degree of mode mixing. A more detailed analysis of the waveguiding properties based on the calculation of the complete set of guided mode profiles and their respective group delays<sup>12</sup> suggests that intermodal diffusion plays a major role in increasing the fiber bandwidth.

Quantitative insight into the modal delay behavior of the PCFs is obtained by measuring their differential mode delay (DMD) characteristics.<sup>1</sup> Here, a 5  $\mu\text{m}$  core diameter single-mode fiber is scanned over the PCF input at a distance of about 10  $\mu\text{m}$  in accordance with Sect. 3.3 of [14]. For each offset position, the impulse response at the output end is recorded with an optical sampling oscilloscope providing an input port compatible to a 62.5  $\mu\text{m}$  multimode fiber. A gain-switched 850 nm single-mode VCSEL delivering pulses with less than 40 ps full width at half maximum is employed for this purpose.<sup>1</sup> Figure 9 illustrates some of the results. It

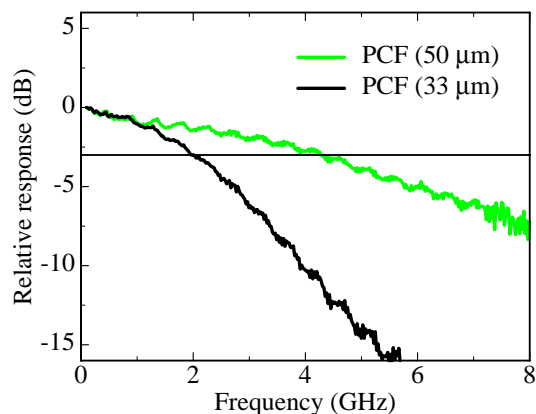


**Figure 8.** Small-signal frequency responses of 100 m-long photonic crystal fibers at 850 nm wavelength.

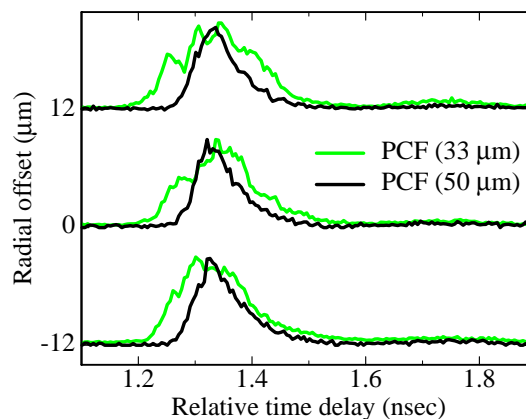


**Figure 9.** Normalized differential mode delay plots for both fibers at offset positions of  $-12$ ,  $0$ , and  $12$   $\mu\text{m}$ .

is apparent that the output pulses of the  $50$   $\mu\text{m}$  fiber are rather narrow and virtually independent of the offset position. On the other hand, those of the  $33$   $\mu\text{m}$  sample show larger variability and are up to twice as broad, which well supports the above observations.

### 4.3. Digital Data Transmission

Data transmission experiments have been carried out under NRZ  $2^7 - 1$  word length PRBS modulation using the aforementioned multimode VCSEL driven with  $V_{pp} = 0.9$  V peak-to-peak voltage. Figure 10 summarizes obtained bit error rate (BER) curves. With the smaller core diameter fiber, up to 5 Gbit/s could be transmitted without indication of a BER floor. The power penalty versus back-to-back (BTB) operation is about 3 dB at a BER of  $10^{-12}$ . On the other hand, the  $50$   $\mu\text{m}$  fiber even enables 10 Gbit/s transmission over 100 m length with only 2.9 dB power penalty. The observed increase in data rate is in full agreement with the small-signal and DMD measurement results.

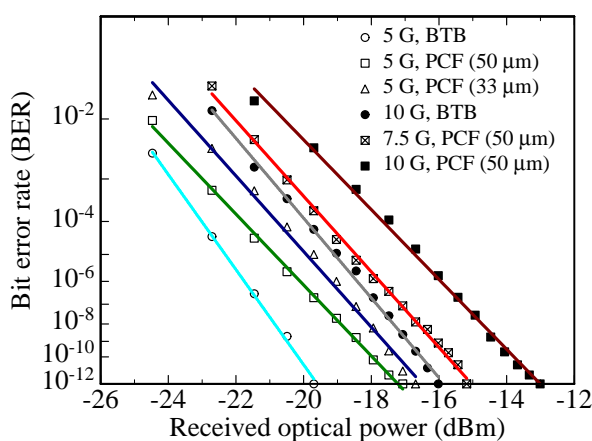


**Figure 10.** BER characteristics for both 100 m-long PCFs at data rates of 5, 7.5, and 10 Gbit/s.

## 5. FSO DATA LINKS BASED ON HIGH-POWER VCSELS

Free-space, “long-distance” optical data transmission is steadily evolving as an attractive application space for short-wavelength VCSELS. Here, lasers with output powers somewhat higher than for fiber-based systems

are employed as convenient sources for inter-window or -rooftop links at Gbit/s data rates and several 100 m interconnection distance.<sup>15</sup> In this section, we will first discuss ongoing experiments using a novel multi-beam transmitter concept and then introduce the static and some dynamic characteristics of next generation high-power VCSELs for FSO applications.

### 5.1. Multi-Beam VCSEL Transmitter Module



**Figure 11.**  $4 \times 4$  VCSEL beam FSO module in a test version (*left*) and integrated into a complete FSO transceiver device (*right*).

In [1] we have discussed the design concept of a free-space optical transmitter module employing multiple VCSEL beams.<sup>16</sup> It consists of a printed circuit board onto which a plurality of driving circuits and lasers is mounted (chip-on-board technology). A plate carrying an identical number of collimating lenses is aligned in front of the board, thus generating a two-dimensional array of laser beams. A single modulation signal is supplied to all VCSELs simultaneously. Compared to available products, such a module is able to provide either increased link availability or transmission distance, or to enable higher bit rates that require higher optical power levels at the receiver. Figure 11 shows a test implementation of a  $4 \times 4$  transmitter module as well as the actual incorporation into a bidirectional FSO device. For an output power per laser of 10 mW, the transmitter conforms to laser class 1M standard IEC 60825-1 (allowing a maximum beam intensity of  $2 \text{ mW/cm}^2$  at 850 nm wavelength) with the chosen 26 mm lens diameter, where the intensity distribution within each beam has to be sufficiently homogeneous. Extensive field tests have been conducted with the 16-beam device from Fig. 11 (right) at the Fast Ethernet bit rate of 125 Mbit/s, with tests at 1.25 Gbit/s planned for the near future. It delivers a record-high class 1M total output power of 160 mW or 22 dBm which translates into a power margin of 30 dB over the chosen 600 m transmission distance. Even for the challenging weather conditions typical for Central Europe, the link availability is then expected to clearly exceed 99%. Over a test period of 3 months the actual availability turned out to be larger than 99.9%, limited by the occurrence of strong fog. The beam divergence angle was adjusted to 6 mrad so that the system does not require automated beam tracking. The receiver side to the right of the transmitter array in Fig. 11 is implemented with a Fresnel lens focusing the light onto a silicon avalanche photodiode, where an interference filter serves to block undesirable background radiation. Stacking of the entire transceiver modules can potentially improve the system performance further. This is due to the fact that beams with larger cross-sectional area on the one hand side increase the power budget and on the other hand side lead to smaller overall variance of the received power since averaging of the uncorrelated optical signal parts takes place in the presence of, e.g., atmospheric scintillation (turbulences).

### 5.2. Large-Area VCSELs for FSO Applications

Figure 12 (left) shows the static operation characteristics of a top-emitting  $25 \mu\text{m}$  active diameter oxide-confined 850 nm VCSEL to be employed in FSO transmitters. The threshold current is 4.5 mA and the slope efficiency amounts to 1 W/A, corresponding to a differential quantum efficiency of  $\eta_d = 68\%$  in the linear power versus current regime. The ohmic resistance is below  $25 \Omega$ .

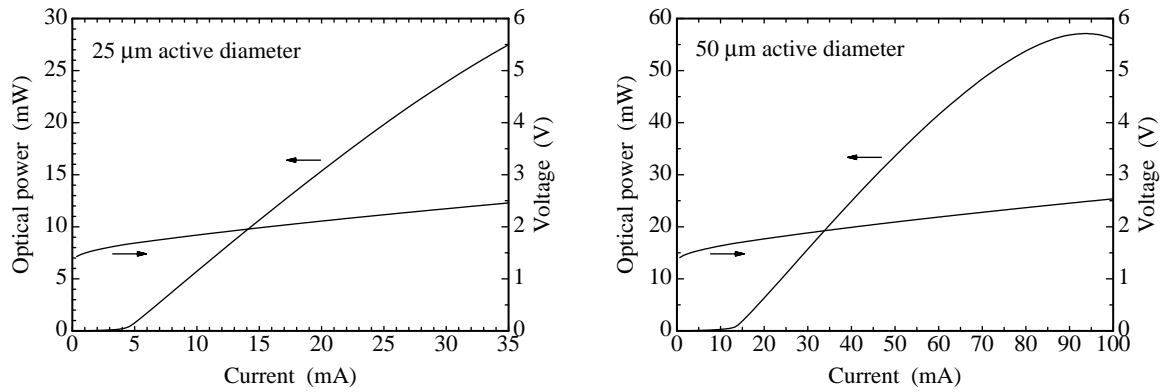


**Figure 12.** Operation characteristics of a top-emitting 25  $\mu\text{m}$  (left) and 50  $\mu\text{m}$  (right) active diameter oxide-confined 850 nm VCSEL.

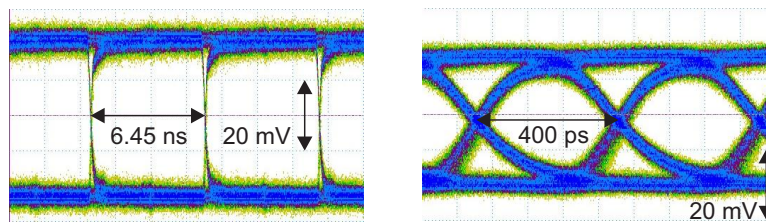


**Figure 13.** Eye diagrams of the 25  $\mu\text{m}$  active diameter VCSEL from Fig. 12.  $B = 155$  Mbit/s data rate,  $I_b = 15$  mA bias current,  $V_{pp} = 1.0$  V peak-to-peak voltage (left) and  $B = 2.5$  Gbit/s,  $I_b = 30$  mA,  $V_{pp} = 2.0$  V (right). In all cases, a 1.87 GHz bandwidth Bessel low-pass filter was used after photodetection.

Optical eye diagrams displayed in Fig. 13 have been taken with the 25  $\mu\text{m}$  VCSEL from Fig. 12 mounted on a TO header that was attached to an SMA socket. A  $50\ \Omega$  output impedance bit pattern generator delivering a  $2^{31} - 1$  word length pseudo-random bit sequence served as the driving source. At the frequently used data rate of 155 Mbit/s, the eye has an almost rectangular shape and even at 2.5 Gbit/s the extinction ratio exceeds 10 dB. At high speed, the eye is somewhat asymmetric owing to longer fall time compared to the rise time. A GaAs-based pin-photodiode with 70  $\mu\text{m}$  diameter and about 8 GHz bandwidth was used at the receiving end.

Operation characteristics of a VCSEL with an even larger active diameter of 50  $\mu\text{m}$  are shown on the right-hand side of Fig. 12. The device features 14 mA threshold current, an initial slope efficiency of 0.94 W/A or  $\eta_d = 64\%$ , a maximum output power of 57 mW at 94 mA current, and a series resistance of  $6\ \Omega$ . A series of eye diagrams taken with the 50  $\mu\text{m}$  VCSEL is displayed in Fig. 14. Whereas at 1.25 Gbit/s data rate, the extinction ratio exceeds 10 dB, it has dropped to about 5 dB at 2.5 Gbit/s modulation. Some distortions of the eyes at high data rates are visible which might be attributed to the non-homogeneous carrier injection through the top ring contact and the associated carrier diffusion-related contributions to the mode dynamics.

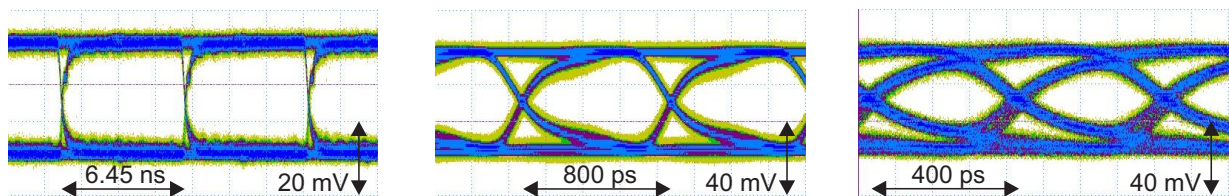


**Figure 14.** Eye diagrams generated by the 50  $\mu\text{m}$  diameter VCSEL from Fig. 12.  $B = 155$  Mbit/s,  $I_b = 30$  mA,  $V_{pp} = 1.0$  V (left) and  $B = 1.25$  Gbit/s (center) as well as  $B = 2.5$  Gbit/s (right), both with  $I_b = 50$  mA,  $V_{pp} = 2.0$  V. Again, the same 1.87 GHz low-pass filter was used in all cases.



**Figure 15.** Photograph of a VCSEL-SMA fiber receptacle before assembly. The 25  $\mu\text{m}$  diameter VCSEL is mounted onto a TO-56 header with a ball lens cap.

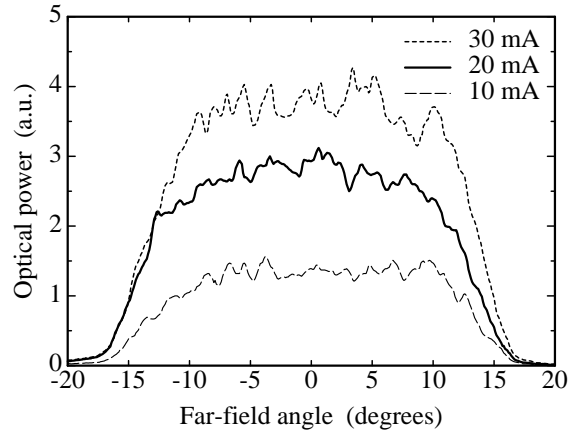


**Figure 16.** Far-field emission patterns of the module from Fig. 15 (with the fiber being attached) for various laser driving currents.

The far-field of a large-area monolithic VCSEL can show a strong center dip due to the predominant excitation of high-order transverse modes. This behavior is often unwanted for FSO applications but can be considerably improved by sending the laser light through a piece of waveguide, thus taking advantage of a mixing effect within the guided modes. Figure 15 shows a photograph of an SMA-type fiber receptacle in which the output of a 25  $\mu\text{m}$  active diameter VCSEL is coupled (by means of a ball lens) into a 125  $\mu\text{m}$  core diameter step-index glass fiber with a numerical aperture of 0.37. In Fig. 16, the far-field patterns as emitted from the fiber end are plotted for different laser driving currents. In order to enhance inter-modal diffusion, the 70 cm-long fiber was wound a single time around a 2 cm diameter rod. The emission characteristic is rather homogeneous and the divergence angle (full width at  $1/e^2$  maximum intensity) of about 31.5 degrees remains almost constant with varying current, which is a favorable feature of an FSO light source.

## 6. CONCLUSIONS

In this paper we have discussed some upcoming application areas for short-wavelength VCSEL-based optical interconnection. We have first reviewed the status of parallel optical interconnect modules. It turns out that although promising results have been presented, the introduction of the next product generation with data rates of 10 Gbit/s per channel might be delayed owing to non-convincing market demand. The extension of the parallel module concept to a two-dimensional array configuration has to rely on matured VCSEL array technology. We have presented flip-chip integrated 2-D arrays capable of 10 Gbit/s operation and featuring reduced internal heating achieved through direct mesa bonding.

As a possible alternative to graded-index fibers in optical datacom environments, we have investigated the data transmission properties of multimode photonic crystal fibers that are potentially easier to fabricate. For the first time, quasi error-free transmission of 10 Gbit/s digital data signals over a PCF with 50  $\mu\text{m}$  core diameter and as much as 100 m length has been demonstrated.

Free-space optics is a particularly attractive and promising application area for higher power VCSELs. We have reported on successful field tests at 125 Mbit/s data rate with a 16-beam transceiver module delivering 160 mW optical power in an eye-safe manner. Large-area VCSELs with tens of milliwatt output power and sufficient modulation speed are under development. We have shown good quality eye diagrams at 2.5 Gbit/s and 1.25 Gbit/s generated by 25  $\mu\text{m}$  and 50  $\mu\text{m}$  active diameter devices, respectively. It was demonstrated that the homogeneity of the far-field pattern can be easily adapted to practical requirements through a fiber pigtail.

## ACKNOWLEDGMENTS

The help of Cristina Goya Herrera and Martin Feneberg with the characterization of the 2-D VCSEL arrays and the high-power VCSELs, respectively, is gratefully acknowledged. This work has been partly supported by the German Research Foundation (DFG).

## REFERENCES

1. R. Michalzik, F. Mederer, H. Roscher, M. Stach, H. Unold, D. Wiedenmann, R. King, M. Grabherr, and E. Kube, "Design and communication applications of short-wavelength VCSELs", in *Materials and Devices for Optical and Wireless Communications*, C.J. Chang-Hasnain, Y. Xia, and K. Iga (Eds.), *Proc. SPIE* **4905**, pp. 310–321, 2002.
2. IEEE Standard 802.3ae<sup>TM</sup>, IEEE, Piscataway, NJ, USA, June 2002.  
See URL <http://grouper.ieee.org/groups/802/3/ae/>.
3. See URL <http://www.paralleloptics.org/>.
4. C. Schuster, C.W. Baks, D.M. Kuchta, Y.H. Kwark, and L. Graham, "Electrical interconnect design and optimization for 120 Gbps parallel optical transmitter module and test station", in *Proc. 7th IEEE Workshop on Signal Propagation on Interconnects*. Siena, Italy, May 2003.
5. A. Schild, H.-M. Rein, J. Müllrich, L. Altenhain, J. Blank, and K. Schrödinger, "High-gain SiGe transimpedance amplifier array for a 12 × 10 Gb/s parallel optical-fiber link", *IEEE J. Solid-State Circuits* **38**, pp. 4–12, 2003.
6. "Picolight and IBM achieve unprecedented bandwidth density for optical data transmission", March 24, 2003. See URL <http://www.picolight.com/news/release25.html>.
7. "ULM-photonics, Primarion, Microsemi and OFS enable next generation of parallel optics interconnects at 10 Gb/s per channel", March 2003. See URL [http://www.ulm-photonics.com/docs/pr/pr\\_press.htm](http://www.ulm-photonics.com/docs/pr/pr_press.htm).
8. C. Wilmsen, H. Temkin, L.A. Coldren (Eds.), *Vertical-Cavity Surface-Emitting Lasers*. Cambridge University Press, Cambridge, UK, 1990.
9. R. King, R. Michalzik, R. Jäger, K.J. Ebeling, R. Annen, and H. Melchior, "32-VCSEL channel CMOS-based transmitter module for Gb/s data rates", in *Vertical-Cavity Surface-Emitting Lasers V*, K.D. Choquette and C. Lei (Eds.), *Proc. SPIE* **4286**, pp. 136–141, 2001.
10. R. Pu, C.W. Wilmsen, K.M. Geib, and K.D. Choquette, "Thermal resistance of VCSELs bonded to integrated circuits", *IEEE Photon. Technol. Lett.* **11**, pp. 1554–1556, 1999.
11. W. Nakwaski and M. Osiński, "Thermal resistance of top-surface-emitting vertical-cavity semiconductor lasers and monolithic two-dimensional arrays", *Electron. Lett.* **28**, pp. 572–574, 1992. Corrected in *Electron. Lett.* **28**, p. 1283, 1992.
12. N.A. Mortensen, M. Stach, J. Broeng, A. Petersson, H.R. Simonsen, and R. Michalzik, "Multi-mode photonic crystal fibers for VCSEL based data transmission", *Optics Express*, 2003, to be published.
13. G.P. Agrawal, *Fiber-Optic Communication Systems*, 2nd ed. J. Wiley & Sons, 1997, p. 27.
14. International Electrotechnical Commission, *IEC 60793-1-49: Optical Fibre – Part 1-49: Measurement methods and test procedures – Differential Mode Delay, Pre-standard*, Jan. 2002.
15. H. Willebrand and B.S. Ghuman, *Free-Space Optics: Enabling Optical Connectivity in Today's Networks*, Sams Publishing, Indianapolis, 2001.
16. E. Kube, C. Ocolai, and F. Ebermann, "Apparatus and method for free-space optical communication", applied for United States Patent, Aug. 2002.